LEGGETT–GARG TEST INEQUALITY WITH SPIN AND FLAVOUR NEUTRINO OSCILLATIONS IN A CONSTANT MAGNETIC FIELD

I.A. Monroy†, S.D. Madrid‡

Universidad Distrital Francisco José de Caldas, Bogota, Colombia

Received 29 May 2025, accepted 9 March 2026, published online 9 June 2026

The Leggett–Garg inequality (LGI), an analogue of Bell's inequality involving correlations of measurements of one observable on a system at different times, stands as one of the hallmark tests of quantum mechanics against classical predictions. In this work, we investigate its implications in the context of neutrino flavour ($\nu_e^{\rm L} \leftrightarrow \nu_\mu^{\rm L}$) and spin ($\nu_e^{\rm L} \leftrightarrow \nu_e^{\rm R}$) oscillations in the presence of a constant transverse magnetic field. For systems with strong magnetic fields, we show that, for both cases, there are length regions ΔL where the LGI is violated, as quantified by the correlator functions K_3 and K_4.

DOI:10.5506/APhysPolB.57.7-A3

1. Introduction

Quantum mechanics describes microscopic systems in terms of the superposition of distinct states associated with the spectra of physical observables. When one measurement of these physical observables is performed on a quantum system, it yields one single outcome, with some probability given by quantum mechanics. This idea highlights the distinction between classical systems and the quantum behavior of microscopic systems, as tested through Bell's and Leggett–Garg inequalities. Bell's inequality concerns correlations among measurements in a spatially entangled system, which is derived by assuming a local hidden-variable theory [1]. The LGI is an analogous test based on temporal correlations of measurements of one observable of a system at different times [2]. Both Bell's and Leggett–Garg inequalities are fulfilled within their *classical* formulation; however, when the correlations are obtained using quantum states, these inequalities are violated and cannot be explained by classical theories.

† iamonroyc@udistrital.edu.co

‡ sdmadridt@udistrital.edu.co

LGI is based on the concept of *macrorealism* (MR) and *non-invasive measurability* (NIM). MR means that the system which has two or more macroscopically distinct states, pertaining to an observable $\hat{Q}$, always exists in one of these states, irrespective of any measurement performed on it. NIM states that we can measure $\hat{Q}$ without disturbing the future dynamics of the system. Given the two-time correlation function $C_{ij} = \langle Q(t_i)Q(t_j)\rangle$ for $t_j > t_i$, with a dichotomous observable $Q = \pm 1$, the two simplest Leggett–Garg functions are given by [2, 3]

$$K_3 = C_{12} + C_{23} - C_{13}\,, \tag{1}$$

$$K_4 = C_{12} + C_{23} + C_{34} - C_{14}\,. \tag{2}$$

It has been established that $-3 \leq K_3 \leq 1$ and $-2 \leq K_4 \leq 2$, but, as discussed above, these inequalities are violated by quantum mechanics.

LGIs have been studied in many works, both theoretically and experimentally [4–11]. Several studies have focused on LGI violations in neutrino systems [12–19]. For the neutrino flavour oscillation in vacuum, as reported in [18], an LGI violation is found with a maximum value of $K_4 = 2.76$, with equal interval times and values of Δm^2, and the mixing angle θ from the KamLAND experimental setup. In addition, it has been found that the maximum value of K_4 depends sensitively on the mixing angle. In [19], it has been demonstrated how oscillation phenomena can be used to test violations of the classical limit by performing measurements on an ensemble of neutrinos at different energies, rather than on a single neutrino at different times. Here, the quantities K_3 and K_4 have been studied as a function of relative phases, yielding a prediction inconsistent with MR at the confidence level of 7σ for K_4, which constitutes a clear observation of LGI violations.

In this work, we study the LGI for neutrino flavour-and-spin oscillations in a constant magnetic field. This provides a suitable framework for exploring quantum aspects in relativistic particle systems in astrophysical contexts. We consider a neutron star, a system with an extreme astrophysical environment and a strong magnetic field.

2. Massive neutrino in a magnetic field

In the initial formulation of the Standard Model, neutrinos are massless particles with no electromagnetic properties. However, in an extension of this model, massive Dirac neutrinos have a non-zero magnetic moment, which implies that neutrinos have non-trivial electromagnetic properties [20, 21]. The magnetic moment of the neutrino mass states is given by [20, 21]

$$\mu_{ii}^{\mathrm{D}} = \frac{3eG_{\mathrm{F}}m_i}{8\sqrt{2}\pi^2} \approx 3.2\times 10^{-19}\left(\frac{m_i}{1\ \mathrm{eV}}\right)\mu_{\mathrm{B}}\,, \tag{3}$$

where μ_{B} is the Bohr magneton. As a consequence of the interaction of the neutrinos' magnetic moment with a transverse magnetic field, phenomena such as spin precession arise, and flavour oscillation patterns are modified. Spin precession causes left-handed neutrinos to become right-handed neutrinos and *vice versa*. A similar change occurs with flavour oscillation. This explains the four neutrino species that correspond to two different flavour states with both right-handed and left-handed helicities.

2.1. Neutrino flavour and spin oscillations in a constant magnetic field

The two neutrino flavour states are given by equations

$$\left|\nu_e^{\mathrm{L(R)}}\right\rangle = \left|\nu_1^{\mathrm{L(R)}}\right\rangle \cos\theta + \left|\nu_2^{\mathrm{L(R)}}\right\rangle \sin\theta\,, \tag{4}$$

$$\left|\nu_\mu^{\mathrm{L(R)}}\right\rangle = -\left|\nu_1^{\mathrm{L(R)}}\right\rangle \sin\theta + \left|\nu_2^{\mathrm{L(R)}}\right\rangle \cos\theta\,, \tag{5}$$

with $\nu_i^{\mathrm{L(R)}}$ as the neutrino mass states helicity ($i = 1, 2$). There are many ways to address neutrino oscillations in a magnetic field [22–25]. However, in this work, we adopt the approach implemented in [26]. As helicity mass states $\nu_i^{\mathrm{L(R)}}$ are not stationary in the presence of a magnetic field, we expand $\nu_i^{\mathrm{L(R)}}$ over the neutrino stationary states $\nu_i^{-(+)}$.

Neutrino states ν_i^s ($s = \pm 1$) of a massive neutrino that propagates along the $\boldsymbol{n}_z$ direction in the presence of a constant and arbitrarily oriented magnetic field can be found as the solution of the Dirac equation

$$\left(\gamma^\mu p_\mu - m - \mu_i \boldsymbol{\Sigma}\cdot\boldsymbol{B}\right)|\nu_i^s(p)\rangle = 0\,, \tag{6}$$

where μ_i is the neutrino magnetic moment and the magnetic field is given by $\boldsymbol{B} = (B_\perp, 0, B_{||})$. Equation (6) can be re-written in the equivalent form

$$\hat{H}_i|\nu_i^s\rangle = E|\nu_i^s\rangle\,, \tag{7}$$

where the Hamiltonian is

$$\hat{H} = \gamma_0\boldsymbol{\gamma}\cdot\boldsymbol{p} + m\gamma_0 + \mu_i\gamma_0\boldsymbol{\Sigma}\cdot\boldsymbol{B}\,. \tag{8}$$

The neutrino energy spectrum is given by

$$E_i^s = \sqrt{m_i^2 + p^2 + \mu_i^2\boldsymbol{B}^2 + 2\mu_i s\sqrt{m_i^2\boldsymbol{B}^2 + p^2 B_\perp^2}}\,, \tag{9}$$

where $s = \pm 1$ corresponds to two different eigenvalues of the Hamiltonian and $p = |\boldsymbol{p}|$. For relativistic neutrino energies, we have $p \gg m$, and for realistic values of the neutrino magnetic moments and magnetic-fields strengths, we also obtain $p \gg \mu B$. With this approximation, the energy values are given by

$$E_i^s \approx p + \frac{m_i^2}{2p} + \frac{\mu_i^2 B^2}{2p} + 2\mu_i s B_\perp \,. \tag{10}$$

The corresponding spin operator that commutes with the neutrino Hamiltonian in the magnetic field (8) can be chosen in the form [26]

$$\hat{S}_i = \frac{1}{N}\left[\boldsymbol{\Sigma}\cdot\boldsymbol{B} - \frac{i}{m_i}\gamma_0\gamma_5(\boldsymbol{\Sigma}\times\boldsymbol{p})\boldsymbol{B}\right] , \tag{11}$$

with

$$\frac{1}{N} = \frac{m_i}{\sqrt{m_i^2\boldsymbol{B}^2 + p^2 B_\perp^2}} \,. \tag{12}$$

For stationary neutrino states, the spin operator $\hat{S}_i$ has to satisfy the equation

$$\hat{S}_i|\nu_i^s\rangle = s|\nu_i^s\rangle \,, \tag{13}$$

with again, $s = \pm 1$ and

$$\left\langle \nu_i^s \middle| \nu_j^{s'} \right\rangle = \delta_{ss'}\delta_{ij} \,. \tag{14}$$

A projector operator is introduced

$$\hat{P}_i^\pm = \frac{1 \pm \hat{S}_i}{2} \,, \tag{15}$$

where for stationary states, $\hat{P}_i^\pm$ must satisfy the eigenvalue equation

$$\left\langle \nu_i^s \middle| \hat{P}_i^\pm \middle| \nu_j^{s'} \right\rangle = \delta_{ss'}\delta_{ij} \,. \tag{16}$$

Neutrino helicity states can be expanded over the neutrino stationary states

$$\left|\nu_i^{\mathrm{L}}(t)\right\rangle = c_i^+ \mathrm{e}^{-iE_i^+ t}\left|\nu_i^+\right\rangle + c_i^- \mathrm{e}^{-iE_i^- t}\left|\nu_i^-\right\rangle , \tag{17}$$

$$\left|\nu_i^{\mathrm{R}}(t)\right\rangle = d_i^+ \mathrm{e}^{-iE_i^+ t}\left|\nu_i^+\right\rangle + d_i^- \mathrm{e}^{-iE_i^- t}\left|\nu_i^-\right\rangle , \tag{18}$$

where $|\nu_i^\pm\rangle$ are stationary eigenstates of the Hamiltonian, and $c_i^\pm, d_i^\pm$ are time-independent coefficients determined from the initial conditions. Since ultrarelativistic neutrinos are produced in weak interaction process always as left-handed helicity states, in this approximation, helicity and chiral states are almost indistinguishable.

The coefficients $c_i^{\pm}$ and $d_i^{\pm}$ are given by the matrix elements of the projector operators (15)

$$\left|c_i^{\pm}\right|^2 = \langle\nu_i^{\mathrm{L}}|\hat{P}_i^{\pm}|\nu_i^{\mathrm{L}}\rangle = \frac{1}{2}\left(1 \pm \frac{B_{||}}{N}\right), \tag{19}$$

$$\left|d_i^{\pm}\right|^2 = \langle\nu_i^{\mathrm{R}}|\hat{P}_i^{\pm}|\nu_i^{\mathrm{R}}\rangle = \frac{1}{2}\left(1 \mp \frac{B_{||}}{N}\right), \tag{20}$$

$$\left(d_i^{\pm}\right)^* c_i^{\pm} = \langle\nu_i^{\mathrm{L}}|\hat{P}_i^{\pm}|\nu_i^{\mathrm{R}}\rangle = \mp\frac{1}{2}\frac{p\left(B_{||} + iB_{\perp}\right)}{m_i N}, \tag{21}$$

and, again $1/N$ is given by Eq. (12). Neutrino stationary states are given by $|\nu_i^s(t)\rangle = \mathrm{e}^{-iE_i^s t}|\nu_i^s(0)\rangle$, from which the flavour states (4) and (5) can be written as

$$\begin{aligned} \left|\nu_e^{\mathrm{L}}(t)\right\rangle &= \left[c_1^+\mathrm{e}^{-iE_1^+t}\left|\nu_1^+\right\rangle + c_1^-\mathrm{e}^{-iE_1^-t}\left|\nu_1^-\right\rangle\right]\cos\theta \\ &\quad + \left[c_2^+\mathrm{e}^{-iE_2^+t}\left|\nu_2^+\right\rangle + c_2^-\mathrm{e}^{-iE_2^-t}\left|\nu_2^-\right\rangle\right]\sin\theta, \end{aligned} \tag{22}$$

$$\begin{aligned} \left|\nu_\mu^{\mathrm{L}}(t)\right\rangle &= -\left[c_1^+\mathrm{e}^{-iE_1^+t}\left|\nu_1^+\right\rangle + c_1^-\mathrm{e}^{-iE_1^-t}\left|\nu_1^-\right\rangle\right]\sin\theta \\ &\quad + \left[c_2^+\mathrm{e}^{-iE_2^+t}\left|\nu_2^+\right\rangle + c_2^-\mathrm{e}^{-iE_2^-t}\left|\nu_2^-\right\rangle\right]\cos\theta, \end{aligned} \tag{23}$$

where, for simplicity, $|\nu_{1,2}^{\pm}\rangle = |\nu_{1,2}^{\pm}(0)\rangle$. The probability of flavour oscillation $\nu_e^{\mathrm{L}} \leftrightarrow \nu_\mu^{\mathrm{L}}$ is given by the expression

$$P_{\nu_\mu^{\mathrm{L}}\to\nu_e^{\mathrm{L}}}(t) = \left|\left\langle\nu_\mu^{\mathrm{L}}(0)\middle|\nu_e^{\mathrm{L}}(t)\right\rangle\right|^2, \tag{24}$$

which, with Eqs. (22) and (23) becomes

$$\begin{aligned} P_{\nu_\mu^{\mathrm{L}}\to\nu_e^{\mathrm{L}}}(t) &= \sin^2\theta\cos^2\theta\Big| - \left|c_1^+\right|^2\mathrm{e}^{-iE_1^+t} - \left|c_1^-\right|^2\mathrm{e}^{-iE_1^-t} \\ &\quad + \left|c_2^+\right|^2\mathrm{e}^{-iE_2^+t} + \left|c_2^-\right|^2\mathrm{e}^{-iE_2^-t}\Big|^2. \end{aligned} \tag{25}$$

The oscillation probability in Eq. (25) has a set of characteristic energies. For simplicity, we consider the case where $\mu_1 = \mu_2 = \mu$. In the ultrarelativistic approximation ($p \gg m$), these characteristic energy values are

$$E_1^+ - E_1^- = E_2^+ - E_2^- = 2\mu B_\perp, \tag{26}$$

$$E_2^+ - E_1^+ = E_2^- - E_1^- = \frac{\Delta m^2}{2p}, \tag{27}$$

$$E_2^- - E_1^+ = \frac{\Delta m^2}{2p} - 2\mu B_\perp, \tag{28}$$

$$E_2^+ - E_1^- = \frac{\Delta m^2}{2p} + 2\mu B_\perp. \tag{29}$$

The probability of flavour oscillation $P_{\nu_\mu^{\rm L}\to\nu_e^{\rm L}}(t)$ is simplified if one accounts for the relativistic neutrino energies ($p \gg m$) and for realistic values of the neutrino magnetic moments and the strengths of magnetic fields ($p \gg \mu B$). In this case, we obtain from Eqs. (19) and (20) that $|c_i^\pm| = |d_i^\pm| \approx 1/2$. Therefore, applying these conditions to the expression in Eq. (25), the probability of flavour oscillations $\nu_\mu^{\rm L} \leftrightarrow \nu_e^{\rm L}$ becomes

$$P_{\nu_\mu^{\rm L}\to\nu_e^{\rm L}}(t) \;=\; \cos^2(\mu B_\perp t)\sin^2 2\theta \sin^2\left(\frac{\Delta m^2}{4p}t\right) . \tag{30}$$

For completeness, the survival relation probability

$$\begin{aligned} P_{\nu_e^{\rm L}\to\nu_e^{\rm L}}(t) \;&=\; \left|\left\langle \nu_e^{\rm L}(0)\middle|\nu_e^{\rm L}(t)\right\rangle\right|^2 \\ &=\; \cos^2(\mu B_\perp t)\left[1-\sin^2 2\theta\sin^2\left(\frac{\Delta m^2}{4p}t\right)\right] \end{aligned} \tag{31}$$

is also calculated. The probability $P_{\nu_\mu^{\rm L}\to\nu_\mu^{\rm L}}$ is analogous to that in Eq. (31). Notice that the probability of finding $\nu_\mu^{\rm L}$ and $\nu_e^{\rm L}$ at time t is not 1, *i.e.*,

$$P_{\nu_\mu^{\rm L}\to\nu_e^{\rm L}}(t) + P_{\nu_\mu^{\rm L}\to\nu_\mu^{\rm L}}(t) = \cos^2(\mu B_\perp t) . \tag{32}$$

This result implies that there will be regions where the probability of finding $\nu_e^{\rm L}$ and $\nu_\mu^{\rm L}$ will be appreciable, *i.e.*, when $P_{\nu_\mu^{\rm L}\to\nu_e^{\rm L}}(t) + P_{\nu_\mu^{\rm L}\to\nu_\mu^{\rm L}}(t) \approx 1$.

The spin oscillation $\nu_e^{\rm L} \leftrightarrow \nu_e^{\rm R}$ probability is given by

$$\begin{aligned} P_{\nu_e^{\rm L}\to\nu_e^{\rm R}}(t) \;&=\; \left|\left\langle \nu_e^{\rm L}(0)\middle|\nu_e^{\rm R}(t)\right\rangle\right|^2 \\ &=\; \sin^2(\mu B_\perp t)\left[1-\sin^2 2\theta\sin^2\left(\frac{\Delta m^2}{4p}t\right)\right] , \end{aligned} \tag{33}$$

which are obtained in a similar way to the probability of flavour oscillation (30).

3. Leggett–Garg inequality for neutrino flavour and spin oscillations in a magnetic field

The correlation function C_{ij} is defined as [3]

$$C_{ij} = \sum_{Q_i,Q_j=\pm1} Q_i Q_j P_{ij}(Q_i,Q_j) . \tag{34}$$

Here, $P_{ij}(Q_i,Q_j)$ represents the joint probability of measuring $Q_i = \pm1$ at time t_i and $Q_j = \pm1$ at time t_j. Most systems in which LGI has been tested use a single observable, but here we can test inequalities using two dichotomous observables, *i.e.*, flavour and spin. We study each case separately here.

3.1. LGI for neutrino flavour oscillation

Let us consider neutrino flavour oscillations in a magnetic field, taking the main system $\nu_e^{\rm L} \to \nu_\mu^{\rm L}$. We take $Q = +1$ when the system is in the $|\nu_e^{\rm L}\rangle$ state and $Q = -1$ when the system is in the $|\nu_\mu^{\rm L}\rangle$ state. The correlation function C_{12} given by Eq. (34) can be expressed in terms of joint probabilities using the notation introduced in [18]. If $|\nu_\mu^{\rm L}\rangle$ is the initial state, we write the joint probability as

$$P_{\nu_\mu^{\rm L}\to\nu_e^{\rm L}}(t_1)P_{\nu_e^{\rm L}\to\nu_e^{\rm L}}(t_2) = P_{\nu_e^{\rm L},\nu_e^{\rm L}}(t_1,t_2)\,, \tag{35}$$

and thus we have the correlation function in terms of four joint probabilities, given by the expression

$$C_{12} = P_{\nu_e^{\rm L},\nu_e^{\rm L}}(t_1,t_2) - P_{\nu_e^{\rm L},\nu_\mu^{\rm L}}(t_1,t_2) - P_{\nu_\mu^{\rm L},\nu_e^{\rm L}}(t_1,t_2) + P_{\nu_\mu^{\rm L},\nu_\mu^{\rm L}}(t_1,t_2)\,. \tag{36}$$

Again, in this context $P_{\nu_e^{\rm L},\nu_e^{\rm L}}(t_1,t_2)$ denotes the joint probability of finding the state $|\nu_e^{\rm L}\rangle$ at t_1 and t_2, and $P_{\nu_e^{\rm L},\nu_\mu^{\rm L}}(t_1,t_2)$ is the joint probability of finding the states $|\nu_e^{\rm L}\rangle$, $|\nu_\mu^{\rm L}\rangle$ at the respective times t_1 and t_2, *etc.*

The flavour oscillation probabilities are given by Eqs. (30) and (31). If $|\nu_\mu^{\rm L}\rangle$ is the initial state, the joint probability of finding the state $|\nu_e^{\rm L}\rangle$ at t_1 and t_2 is

$$\begin{aligned} P_{\nu_e^{\rm L},\nu_e^{\rm L}}(t_1,t_2) \;&=\; \sin^2 2\theta \sin^2\left(\frac{\Delta m^2}{4p}t_1\right)\cos^2[\mu B_\perp t_1] \\ &\quad\times\left[1-\sin^2 2\theta\sin^2\left(\frac{\Delta m^2}{4p}\Delta t\right)\right]\cos^2(\mu B_\perp \Delta t)\,, \end{aligned} \tag{37}$$

where $\Delta t = t_2 - t_1$. The remaining three joint probabilities can be calculated in a similar way. The above allows us to determine the correlation function C_{12}

$$C_{12} = \cos^2(\mu B_\perp t_1)\cos^2(\mu B_\perp \Delta t)\left[1-2\sin^2 2\theta\sin^2\left(\frac{\Delta m^2}{4p}\Delta t\right)\right]. \tag{38}$$

Notice that C_{12} no longer depends on t_1 when $B_\perp = 0$, but there can still be values of Δt for which $C_{12} \neq 0$. The correlation functions C_{23}, C_{34}, C_{13}, and C_{14} are calculated similarly to Eq. (38), as in the calculation of the functions K_3 and K_4 in Eqs. (1) and (2). We assume equal time intervals between measurements for all correlation functions, *i.e.*, $t_4 - t_3 = t_3 - t_2 = t_2 - t_1 = \Delta t$. This gives $t_2 = t_1 + \Delta t$ and $t_3 = t_1 + 2\Delta t$, which is important for calculating C_{ij} and subsequently the K_3 and K_4 functions. They are written in terms of a distance function using the relativistic limit $t \simeq L$.

Therefore, L_1 and ΔL represent the distances traveled by the neutrinos in time t_1 and interval Δt, respectively. The final results for the functions K_3 and K_4 of the neutrino flavour oscillation are

$$\begin{aligned} K_3 \;=\; & \cos^2(\mu B_\perp \Delta L)\Big[\cos^2(\mu B_\perp L_1) + \cos^2\{\mu B_\perp (L_1+\Delta L)\}\Big] \\ & \times \left[1 - 2\sin^2 2\theta \sin^2\left(\frac{\Delta m^2}{4p}\Delta L\right)\right] \\ & - \cos^2(\mu B L_1)\cos^2(2\mu B_\perp \Delta L)\left[1 - 2\sin^2 2\theta \sin^2\left(\frac{\Delta m^2}{4p}2\Delta L\right)\right], \end{aligned} \tag{39}$$

$$\begin{aligned} K_4 \;=\; & \Big[\cos^2(\mu B_\perp L_1) + \cos^2\{\mu B_\perp (L_1+\Delta L)\} + \cos^2\{\mu B_\perp (L_1+2\Delta L)\}\Big] \\ & \times \cos^2(\mu B_\perp \Delta L)\left[1 - 2\sin^2 2\theta \sin^2\left(\frac{\Delta m^2}{4p}\Delta L\right)\right] \\ & - \cos^2(\mu B_\perp L_1)\cos^2(3\mu B_\perp \Delta L)\left[1 - 2\sin^2 2\theta \sin^2\left(\frac{\Delta m^2}{4p}3\Delta L\right)\right]. \end{aligned} \tag{40}$$

As special cases, when $B_\perp = 0$, Eq. (40) reduces to

$$K_4 = 2 - 2\sin^2 2\theta\left[3\sin^2\left(\frac{\Delta m^2}{4p}\Delta L\right) - \sin^2\left(\frac{\Delta m^2}{4p}3\Delta L\right)\right], \tag{41}$$

which is the usual LGI for vacuum neutrino flavour oscillation studied in [18]. The experimental values of Δm^2 and θ, taken from the KamLAND experiment, are 7.58×10^{-5} eV^2 and 36.80°, respectively [27]. The Standard Model prediction (3) for the magnetic moment is $\mu \sim 10^{-19}\mu_{\mathrm{B}}$ for a neutrino mass of $m = 0.5$ eV.

Several options for L_1 can be chosen; however, we find that LGI violation occurs only when L_1 lies within length intervals where the probability of oscillation is appreciable. This is given by the oscillation length $L + \Delta L = 1/(\mu B)$. For a neutron star, such as magnetar [28], whose size is $L \sim 20$ km and magnetic field values $B \sim 10^{12}$–10^{15} T, we can extend our study of LGIs to this kind of system. In Figs. 1 (a) and 2 (a), we show the plots of the K_3 and K_4 functions for neutrino flavour oscillations in a transverse magnetic field with $B_\perp = 10^{12}$ T, a distance $L_1 = 0$ km, and neutrino energy $p = 1$ MeV. These values generate a length oscillation $\Delta L = 1/(\mu B) \sim 30$ km, which is of the order of a magnetar's size. Both functions display regions where flavour oscillations lead to violations of the LGI. In Figs. 1 (b) and 2 (b), we show plots for K_3 and K_4 functions for cases with and without magnetic field, but within a smaller length region, *i.e.*, a region of size comparable to the neutron star where LGIs are violated. We observe an interesting behavior of the LGIs when the magnetic field is non-zero: there are values of ΔL, where the LGI is not violated when $B \neq 0$; however, in these same regions, the LGI is violated when $B = 0$.

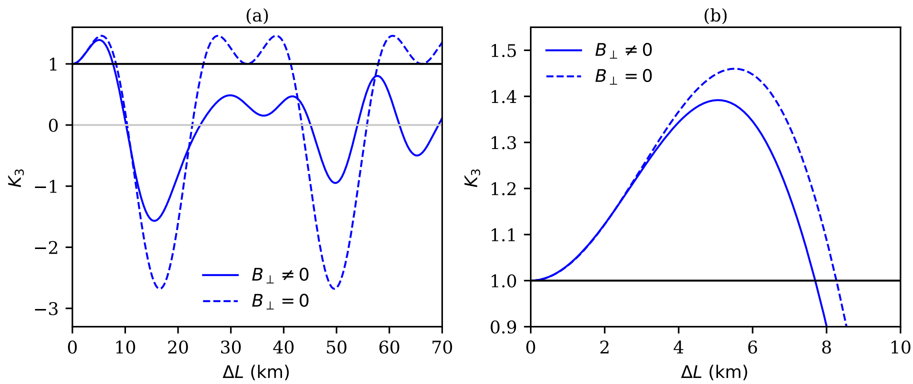

Fig. 1. (a) K_3 plot for the flavour oscillation in a transverse magnetic field $B = 10^{12}$ T, a neutrino energy $p = 1$ MeV, $\Delta m^2 = 7.58 \times 10^{-5}$ eV^2, a magnetic moment $\mu = 10^{-19}\mu_{\rm B}$, and a mixing angle $\theta = 36.80°$. The horizontal black line denotes the maximum value of K_3 allowed by LGI. (b) K_3 for the flavour oscillation within a smaller length region, where $K_3 > 1$, $B_\perp = 0$, and $B_\perp \neq 0$.

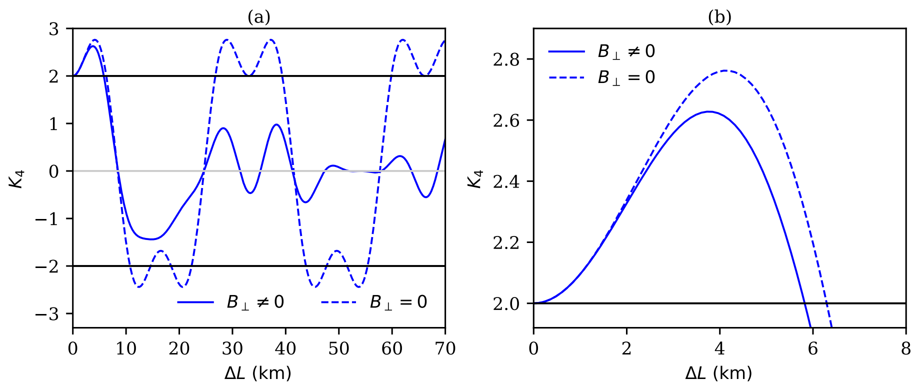

Fig. 2. (a) Plot of K_4 for the flavour oscillation in a transverse magnetic field $B = 10^{12}$ T, a neutrino energy $p = 1$ MeV, $\Delta m^2 = 7.58 \times 10^{-5}$ eV^2, a magnetic moment $\mu = 10^{-19}\mu_{\rm B}$, and a mixing angle $\theta = 36.80°$. Horizontal black lines denote the maximum and minimum values of K_4 allowed by LGI. (b) K_4 for the flavour oscillation within a smaller length region, where $K_4 > 2$, $B_\perp = 0$, and $B_\perp \neq 0$.

Within the plotted range of ΔL, a maximum peak appears in both K_3 and K_4. Specifically, the maximum values attained within the length region from 0 to 70 km are $K_3 = 1.39$ and $K_4 = 2.62$, occurring at $\Delta L = 5.06$ km and $\Delta L = 3.76$ km, respectively. Notably, all these regions in which LGIs are violated lie within the magnetar's size order of magnitude. For comparison, in the zero-field case, the maximum values reached are $K_3 = 1.46$ and $K_4 = 2.76$. In addition, LGIs are violated over larger length intervals. For instance, we obtain $K_3 = 1.42$ at $\Delta L = 104.80$ km and $K_4 = 2.52$ at $\Delta L = 103.50$ km; however, these lengths are significantly larger than the magnetar size.

Let us consider the case where $\Delta m^2 = 0$. In this scenario, there will obviously be no flavour oscillation, and Eq. (41), when the field is zero, indicates that we remain in the classical regime, with $K_4 = 2$. However, if we instead set $\Delta m^2 = 0$ in Eqs. (39) and (40), where the magnetic field remains non-zero, an LGI violation still persists with maximum values of $K_3 = 1.08$ for $\Delta L = 14.50$ km and $K_4 = 2.02$ for $\Delta L = 6.46$ km. In [15], where the LGI for three-flavour neutrino oscillations was studied, the authors also examined the case $\Delta m^2 = 0$ and found an LGI violation. This result can be explained by the fact that, for three-state neutrino oscillations, there are three neutrino mass states, and if two of them become equal, then there will be the possibility of neutrino oscillations because there are now effectively two masses. In our case, the violation of the LGI when $\Delta m^2 = 0$ is explained by the fact that although the flavour transition probability is zero, the survival probability is still non-zero. This indicates that, if we consider $|\nu_\mu^{\mathrm{L}}\rangle$ as the initial state, the probability of detecting $|\nu_e^{\mathrm{L}}\rangle$ is zero. However, the probability of finding $|\nu_\mu^{\mathrm{L}}\rangle$ is not equal to 1, as stated in Eqs. (30) and (31). This implies that measurements of the initial state $|\nu_\mu^{\mathrm{L}}\rangle$ are not trivial. Thus, LGI violation when $\Delta m^2 = 0$ can be clearly attributed to the influence of the magnetic field on the probabilities of flavour oscillation.

Although the present analysis has been restricted to the two-flavour approximation, it is important to note how the situation changes when the full three-flavour framework is considered. The behavior of three-flavour oscillations in a magnetic field reproduces the qualitative effects observed in the two-flavour case [29]; namely, the magnetic field modulates the vacuum oscillation probabilities. However, both two- and three-flavour systems possess their own dynamical structure, so their quantitative evolution differs, even though the qualitative behavior of K_3 and K_4 remains similar.

Moreover, in the three-flavour case, the mixing matrix involves three mixing angles and one complex phase that introduces possible CP-violating effects, which may modify the temporal correlations relevant to the LGI. For instance, Ref. [15] reported that the presence of the CP-violating phase δ_{CP}

can enhance the maximum violation of the LGI, indicating that CP violation may strengthen the quantum nature of the three-flavour neutrino oscillation system [15].

3.2. LGI for neutrino spin oscillation

For neutrino spin oscillations in a magnetic field, we take the main system to be the $\nu_e^{\mathrm{L}} \to \nu_e^{\mathrm{R}}$ system. The spin oscillation probabilities are given by Eqs. (33) and (31). We assign $Q = +1$ when the system is in the $|\nu_e^{\mathrm{R}}\rangle$ state and $Q = -1$ when it is in the $|\nu_e^{\mathrm{L}}\rangle$ state.

In the same way as described in Section 3.1, the correlation function C_{12} is expressed in terms of the four joint probabilities $P_{\nu_e^{\mathrm{R}},\nu_e^{\mathrm{R}}}(t_1,t_2)$, $P_{\nu_e^{\mathrm{R}},\nu_e^{\mathrm{L}}}(t_1,t_2)$, $P_{\nu_e^{\mathrm{L}},\nu_e^{\mathrm{R}}}(t_1,t_2)$, and $P_{\nu_e^{\mathrm{L}},\nu_e^{\mathrm{L}}}(t_1,t_2)$, which can be calculated similarly to the case of flavour oscillations. Therefore, the time-dependent function C_{12} obtained in this case is given by

$$\begin{aligned} C_{12} &= \left(1 - 2\sin^2(\mu B_\perp \Delta L)\right)\left[1 - \sin^2 2\theta \sin^2\left(\frac{\Delta m^2}{4p}L_1\right)\right] \\ &\quad \times \left[1 - \sin^2 2\theta \sin^2\left(\frac{\Delta m^2}{4p}\Delta L\right)\right]. \end{aligned} \tag{42}$$

Applying the same procedure described in Section 3.1, the functions K_3 and K_4 are obtained straightforwardly, and their corresponding results are

$$\begin{aligned} K_3 &= \left[2 - \sin^2 2\theta \sin^2\left(\frac{\Delta m^2}{4p}L_1\right) - \sin^2 2\theta \sin^2\left(\frac{\Delta m^2}{4p}(L_1 + \Delta L)\right)\right] \\ &\quad \times \left(1 - 2\sin^2(\mu B_\perp \Delta L)\right)\left[1 - \sin^2 2\theta \sin^2\left(\frac{\Delta m^2}{4p}\Delta L\right)\right] \\ &\quad - \left(1 - 2\sin^2(2\mu B_\perp \Delta L)\right)\left[1 - \sin^2 2\theta \sin^2\left(\frac{\Delta m^2}{4p}L_1\right)\right] \\ &\quad \times \left[1 - \sin^2 2\theta \sin^2\left(\frac{\Delta m^2}{4p}2\Delta L\right)\right], \end{aligned} \tag{43}$$

$$\begin{aligned} K_4 \;=\; & \left(1-2\sin^2(\mu B_\perp \Delta L)\right)\left[1-\sin^2 2\theta \sin^2\left(\frac{\Delta m^2}{4p}\Delta L\right)\right] \\ & \left[3-\sin^2 2\theta\sin^2\left(\frac{\Delta m^2}{4p}L_1\right)-\sin^2 2\theta\sin^2\left(\frac{\Delta m^2}{4p}(L_1+\Delta L)\right)\right. \\ & \left. -\sin^2 2\theta \sin^2\left(\frac{\Delta m^2}{4p}(L_1+2\Delta L)\right)\right] \\ & -\left(1-2\sin^2(\mu B_\perp 3\Delta L)\right)\left[1-\sin^2 2\theta\sin^2\left(\frac{\Delta m^2}{4p}3\Delta L\right)\right] \\ & \times\left[1-\sin^2 2\theta \sin^2\left(\frac{\Delta m^2}{4p}L_1\right)\right]. \end{aligned} \tag{44}$$

In Figs. 3 and 4, we show the plots of the K_3 and K_4 functions for neutrino spin oscillations using the same values as in Section 3.1 for p, B, μ, and Δm^2. Regions where the LGI is violated can be identified. The maximum LGI violation values obtained in the plotted region are $K_3 = 1.08$ at $\Delta L = 4.02$ km and $K_4 = 2.08$ at $\Delta L = 2.03$ km. Moreover, the LGI is violated over larger length intervals; for example, we obtain $K_3 = 1.28$ for $\Delta L = 97.51$ km and $K_4 = 2.63$ for $\Delta L = 98.62$ km. As a special case, we consider the situation where $\Delta m^2 = 0$. Here again, the LGI violation persists alongside the flavour oscillations, as can be seen in Figs. 3 (a) and 4 (a). A maximum LGI violation occurs at $K_3 = 1.5$ and $K_4 = 2.82$. Finally, we consider the case where we set $B_\perp = 0$ in Eqs. (43) and (44) for K_3 and K_4. Here, we get a violation of the LGI, with, *e.g.*, $K_3 = 1.06$ for $\Delta L = 4.29$ km

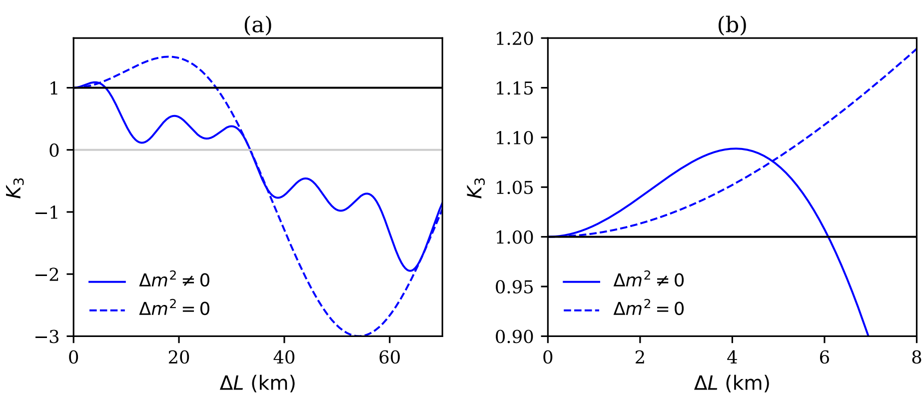

Fig. 3. (a) K_3 plot for the spin oscillation in a transverse magnetic field $B = 10^{12}$ T, a neutrino energy $p = 1$ MeV, $\Delta m^2 = 7.58 \times 10^{-5}$ eV^2, a magnetic moment $\mu = 10^{-19}\mu_{\mathrm{B}}$, and a mixing angle $\theta = 36.80°$. The horizontal black line denotes the maximum value of K_3 allowed by LGI. (b) K_3 for the spin oscillation with a smaller length region, where $K_3 > 1$, $\Delta m = 0$, and $\Delta m \neq 0$.

and $K_4 = 2.01$ for $\Delta L = 1.73$ km. Again, this situation is analogous to flavour oscillations with $\Delta m^2 = 0$, with the distinction that in this case, the violation arises from the dependence of the spin–oscillation probabilities on Δm^2.

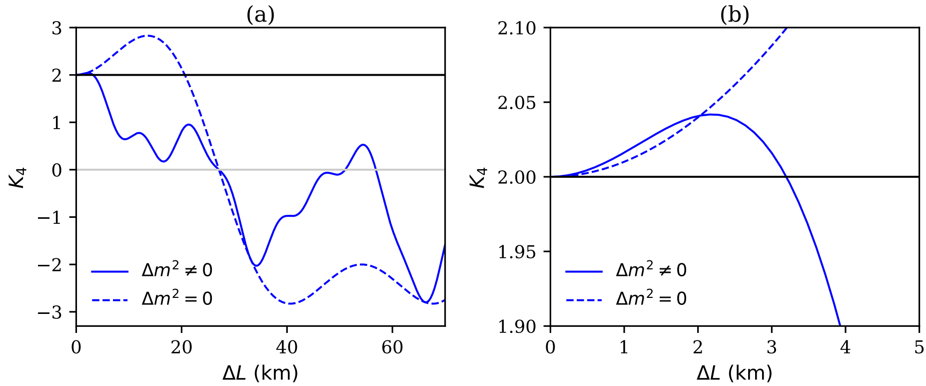

Fig. 4. (a) K_4 plot for the spin oscillation in a transverse magnetic field $B = 10^{12}$ T, a neutrino energy $p = 1$ MeV, $\Delta m^2 = 7.58 \times 10^{-5}$ eV^2, a magnetic moment $\mu = 10^{-19}\mu_{\mathrm{B}}$, and a mixing angle $\theta = 36.80°$. Horizontal black lines denote the maximum and minimum values of K_4. (b) K_4 for spin oscillation within a smaller length region, where $K_4 > 2$, $\Delta m = 0$, and $\Delta m \neq 0$.

4. Conclusions

We studied the LGIs for the cases of neutrino flavour oscillations, $\nu_e^{\mathrm{L}} \leftrightarrow \nu_\mu^{\mathrm{L}}$, and spin oscillations, $\nu_e^{\mathrm{L}} \leftrightarrow \nu_e^{\mathrm{R}}$, in the presence of a constant magnetic field through the K_3 and K_4 functions. We determined that these functions exhibit ΔL regions where LGI violations occur. For flavour oscillations, we found maximum values of $K_3 = 1.39$ and $K_4 = 2.62$, whereas for spin oscillations, we obtained $K_3 = 1.08$ and $K_4 = 2.08$. As special cases, we also studied the regime with $\Delta m^2 = 0$ and again identified regions where LGI violations persist, finding maximum values of $K_3 = 1.08$ and $K_4 = 2.02$ for flavour oscillations, and $K_3 = 1.5$ and $K_4 = 2.82$ for spin oscillations. It is worth highlighting that all the scenarios investigated here correspond to systems with strong magnetic fields, such as the extreme astrophysical environments discussed in [26]. In this context, magnetars are systems to which the results obtained here for neutrino oscillations can be applied. Finally, in the case of a vanishing magnetic field, we also identified ΔL intervals where the K_3 and K_4 functions violate the LGIs for flavour oscillations (as studied in [19]), and additionally for spin oscillations — an aspect less commonly explored in neutrino theory.

REFERENCES

[1] J.S. Bell, «On the Einstein Podolsky Rosen paradox», *Physics* **1**, 195 (1964).

[2] A.J. Leggett, A. Garg, «Quantum mechanics *versus* macroscopic realism: Is the flux there when nobody looks?», *Phys. Rev. Lett.* **54**, 857 (1985).

[3] C. Emary, N. Lambert, F. Nori, «Leggett–Garg inequalities», *Rep. Prog. Phys.* **77**, 016001 (2014); *Corrigendum ibid.* **77**, 039501 (2014).

[4] J. Naikoo, A.K. Alok, S. Banerjee, «Study of temporal quantum correlations in decohering B and K meson systems», *Phys. Rev. D* **97**, 053008 (2018).

[5] K. Sharma, A. Mahapatra, P.K. Panigrahi, S. Patra, «Imprints of LGI violation in mesons», *Eur. Phys. J. Plus* **139**, 1 (2024).

[6] L. Rosales-Zárate, B. Opanchuk, Q.Y. He, M.D. Reid, «Leggett–Garg tests of macrorealism for bosonic systems including double-well Bose–Einstein condensates and atom interferometers», *Phys. Rev. A* **97**, 042114 (2018).

[7] N. Lambert, R. Johansson, F. Nori, «Macrorealism inequality for optoelectromechanical systems», *Phys. Rev. B* **84**, 245421 (2011).

[8] C. Budroni, C. Emary, «Temporal Quantum Correlations and Leggett–Garg Inequalities in Multilevel Systems», *Phys. Rev. Lett.* **113**, 050401 (2014).

[9] M.E. Goggin *et al.*, «Violation of the Leggett–Garg inequality with weak measurements of photons», *Proc. Natl. Acad. Sci. USA* **108**, 1256 (2011).

[10] G.C. Knee *et al.*, «Violation of a Leggett–Garg inequality with ideal non-invasive measurements», *Nat. Commun.* **3**, 606 (2012).

[11] H. Katiyar, A. Brodutch, D. Lu, R. Laflamme, «Experimental violation of the Leggett–Garg inequality in a three-level system», *New J. Phys.* **19**, 023033 (2017).

[12] J.S. Xu, C.F. Li, X.B. Zou, G.C. Guo, «Experimental violation of the Leggett–Garg inequality under decoherence», *Sci. Rep.* **1**, 101 (2011).

[13] M. Blasone, F. Illuminati, L. Petruzziello, L. Smaldone, «Leggett–Garg inequalities in the quantum field theory of neutrino oscillations», *Phys. Rev. A* **108**, 032210 (2023).

[14] X.Z. Wang, B.Q. Ma, «New test of neutrino oscillation coherence with Leggett–Garg inequality», *Eur. Phys. J. C* **82**, 133 (2022).

[15] D. Gangopadhyay, A.S. Roy, «Three-flavoured neutrino oscillations and the Leggett–Garg inequality», *Eur. Phys. J. C* **77**, 260 (2017).

[16] Q. Fu, X. Chen, «Testing violation of the Leggett–Garg-type inequality in neutrino oscillations of the Daya Bay experiment», *Eur. Phys. J. C* **77**, 775 (2017).

[17] S. Shafaq, T. Kushwaha, P. Mehta, «Investigating Leggett–Garg inequality in neutrino oscillations — role of decoherence and decay», `arXiv:2112.12726 [hep-ph]`.

[18] D. Gangopadhyay, D. Home, A. Sinha Roy, «Probing the Leggett–Garg inequality for oscillating neutral kaons and neutrinos», *Phys. Rev. A* **88**, 022115 (2013).

[19] J.A. Formaggio, D.I. Kaiser, M.M. Murskyj, T.E. Weiss, «Violation of the Leggett–Garg Inequality in Neutrino Oscillations», *Phys. Rev. Lett.* **117**, 050402 (2016).

[20] K. Fujikawa, R. Shrock, «Magnetic Moment of a Massive Neutrino and Neutrino-Spin Rotation», *Phys. Rev. Lett.* **45**, 963 (1980).

[21] A. Studenikin, «Neutrino electromagnetic properties: a window to new physics — II», *PoS* **(EPS-HEP2017)**, 137 (2017).

[22] J. Schechter, J.W.F. Valle, «Majorana neutrinos and magnetic fields», *Phys. Rev. D* **24**, 1883 (1981).

[23] L. Okun, M. Voloshin, M. Vysotsky, «Neutrino electrodynamics and possible consequences for solar neutrinos», *Sov. Phys. JETP* **64**, 446 (1986), `http://jetp.ras.ru/cgi-bin/dn/e_064_03_0446.pdf`

[24] E. Akhmedov, «Resonant amplification of neutrino spin rotation in matter and the solar-neutrino problem», *Phys. Lett. B* **213**, 64 (1988).

[25] C.-S. Lim, W. Marciano, «Resonant spin-flavour precession of solar and supernova neutrinos», *Phys. Rev. D* **37**, 1368 (1988).

[26] A. Popov, A. Studenikin, «Neutrino eigenstates and flavour, spin and spin-flavour oscillations in a constant magnetic field», *Eur. Phys. J. C* **79**, 144 (2019).

[27] S. Abe *et al.*, «Precision Measurement of Neutrino Oscillation Parameters with KamLAND», *Phys. Rev. Lett.* **100**, 221803 (2008).

[28] V.M. Kaspi, A. Beloborodov, «Magnetars», *Annu. Rev. Astron. Astrophys.* **55**, 261 (2017).

[29] A. Lichkunov, A. Popov, A. Studenikin, «Three-flavour neutrino oscillations in a magnetic field», *Int. J. Mod. Phys. A* **41**, 2650015 (2026), `arXiv:2207.12285 [hep-ph]`.